Earth Planets Space, **62**, 91–98, 2010

The influence of particle shapes and sizes in the CO ice stretching mode

R. Vilaplana[1], J. Canto[1], F. Moreno-Danvila[2], and D. Guirado[2]

[1]*Universidad Politécnica de Valencia, Applied Physics Dept., Placeta Ferrándiz y Carbonell, n° 2, 03801 Alcoy (Alicante), Spain*
[2]*Instituto de Astrofísica de Andalucía (CSIC), Solar System Dept., C/ Camino Bajo de Huetor, n° 50, 18008 Granada, Spain*

(Received July 31, 2008; Revised June 20, 2009; Accepted July 16, 2009; Online published February 12, 2010)

Ices are major components of dust grains in the interstellar medium, with H_2O, CO, and CO_2 ices being the most ubiquitous. We have studied the influence of particle shapes and sizes on the profile of the CO ice stretching mode by means of computational calculations. The extinction factors were calculated using Mie and DDA codes for a number of shapes and size parameters, ranging from the Rayleigh regime up to 3. A scattering peak displaced towards the reddish wavelength for size parameters larger than 1 was observed in all cases considered, independently of the ice (CO and CO_2), the shapes (sphere, spheroid with axial proportion 5, DW1999, and aggregates), and the inclusion of other constituents, such as silicate. We have attributed this fact to the grain growth. Certain shapes also produced a double-peaked profile but in the wavelength range in which the surface modes can be observed. The calculations, including those for silicate, show a decrease in the band strength but the changes in the stretching mode profile of CO ice are not significant.
Key words: Dust, grain growth, CO ice stretching mode, IMS: extinction-infrared.

1. Introduction

Ices are major components of dust grains, influencing the chemical and physical processes in the interstellar medium (ISM). In this field, spectroscopic methods play a crucial role. Our knowledge of ice processes is mainly inferred from comparisons between spectral observations and spectral measurements in the laboratory. Some of the most ubiquitous interstellar ices are those of H_2O, CO, and CO_2. Infrared (IR) observations of some of their main bands show different profiles depending on the line of sight. These profiles and their positions can be influenced by different factors, such as the molecular environment (Hudgins *et al*., 1993; Ehrenfreund *et al*., 1996), the temperature (Schmitt *et al*., 1989; Smith *et al*., 1994; Raut *et al*., 2004), the irradiation history (Palumbo, 2006; Fama *et al*., 2008), and the particle shapes and sizes (Dartois *et al*., 2003; Dartois, 2006). In the laboratory, ice spectra are generally obtained from films formed by deposition at low temperature on a flat substrate, while ices in molecular clouds grow and form mantles covering the small core grains or form heterogeneous mixtures (ice/silicates/carbonaceous material) by coagulation in a volume or aggregates. In view of this, it is important to study how the particle shapes and sizes influence the profile of these bands. Here, we have focused our attention on the stretching mode of CO ice.

Historically, observations of the stretching mode of CO ice along many lines of sight have revealed decomposition into a broader red-shifted component situated somewhere in the region 2130–2138 cm^{-1} (red component) and a narrow component centred on 2140 cm^{-1} (middle component) (Lacy *et al*., 1884; Whittet *et al*., 1985; Geballe, 1986). However, recent surveys of low-mass stars have also shown the presence of a third narrow band at 2143 cm^{-1} (blue component) (Pontoppidan *et al*., 2003). Laboratory measurements on CO mixtures with other gases deposited on a flat substrate at low temperature have shown that the middle component occurs in mixtures dominated by non-polar molecules (CO_2, O_2, N_2) and that a broader reddish component appears in mixtures dominated by polar molecules, such as H_2O, NH_3 and CH_3OH (Tielens *et al*., 1991; Palumbo *et al*., 1995; Ehrenfreund *et al*., 1996, 1997). Conversely, recent spectral measurements have been made at low temperatures of crystalline CO ice clusters generated by the collisional-cooling technique; apart from their application to aerosols, these are of interest because, contrary to what happens with the ice spectral measurements on a flat substrate, the shape effects are included in these spectra.

In the following, we describe several studies in detail that have especially focused on investigating the stretching mode of CO ice.

Tielens *et al*. (1991) measured the deposition of CO ices and its mixtures on a flat substrate. In their measurements, both pure CO ice and mixtures with polar and non-polar ices were considered. These researchers observed a narrow CO band (middle component) in mixtures dominated by non-polar molecules and a broader reddish one in mixtures dominated by polar ices (essentially H_2O). In an attempt to understand the possible influence of particle shape and size on the stretching mode of the CO ice, they carried out a number of computational calculations in the Rayleigh regime, obtaining the absorption cross section for various single CO ice shapes (spheres, prolate, and oblate spheroids, rods, and

doi:10.5047/eps.2009.07.001

disks). They found that while the CO ice spheres show a single profile, the rest of these CO ice shapes show a double-peaked profile. In order to mimic the diffuse ISM in a more accurate way, these authors modelled the dust grain by means of core-mantle spheres or spheroids and also observed the double-peaked profile. They found that size and shape distributions tend to smooth out the spectral substructures (double-peaked). In an attempt to mimic the effect of the grain growth in dense clouds, they extended the lower and upper size distribution limits and observed an increasing importance of scattering as evidenced by the rise in the scattering peak: it was slightly displaced from the absorption peak to a higher wavelength.

Dartois (2006) carried out computational calculations of the volume attenuation coefficient for spherical and ellipsoidal coated grains (CO ice mantle and silicate core, CO ice mantle and carbonaceous core, double-coated CO and H_2O ices, and silicate core) from different relative core-mantle volume fractions and size parameters up to 10. He also used the effective medium theory (EMT) in two cases: (1) ellipsoid with inclusions of ice in all the volumes in an attempt to consider a best model for larger grains; (2) coated ellipsoids with a mantle of 50% of CO ice with a porosity degree of 50%. The results obtained with core-mantle models (spheres or ellipsoids) revealed that the appearance of a substructure (double-peaked) in the Rayleigh regime depends on the relative core-mantle volume fraction. Nevertheless, the results with EMT did not show this substructure. Moreover, when he included non-Rayleigh particles in the distribution, a scattering peak slightly displaced from the absorption one was observed for all cases. This observation led Dartois to suggest that grain growth could be a complementary explanation of the large red component observed along many lines of sight tracing the scattering degree affecting the CO ice stretching mode profile.

Dartois and Bauerecker (2008) studied infrared crystalline CO ice clusters (generated with the collisional cooling technique) in the aerosol phase at temperatures between 5 and 35 K and sizes ranging from 10 to 1000 nm. They observed different profiles in their spectra. The larger clusters enabled them to determine the CO ice optical constants, free of substrate interfaces and complementary to thin films. Using these optical constants and the DDA method, they obtained the extinction spectra for parallelepiped shapes with various edges ratios. Numerous substructures were observed depending on the specific particle shapes. These researchers used these results to predict the shape effects on the spectra and the nucleation tendencies. They also calculated the extinction factors of the CO ice for different particle shapes in the Rayleigh regime (sphere, cube, needle, and disk) and compared them with one spectrum of the CO ice cluster and with one spectrum of pure CO ice film. They found that the spectrum of the CO cluster was better represented by a spherical shape, whereas that of the CO ice film was best fitted by a disk shape. Finally, they also tested the effect of bigger sizes by calculating the volume attenuation coefficient for CO ice spheres and obtained their own optical constants. These authors concluded that the scattering portion of the spectrum increases when bigger sizes are included, illustrating that this predominantly occurs around 2137 cm^{-1}, at lower wavenumbers of the LO–TO range.

In order to shed some light on the problem of how particle shape and size influences the stretching mode profile of CO ice, we have calculated the extinction factors using Mie and DDA codes for a number of shapes with size parameters varying from the Rayleigh regime up to 3. In the following sections, we will refer size parameter to the volume-equivalent size parameter of the particle and denote it as "X". The starting point of our calculations considers particles with only ice as a constituent. Clearly, the dust grain is not well represented by such. For small grains, it would be more realistic to use a core-mantle model. Moreover, if the coagulation process dominates the formation of the dust grains in dense molecular clouds (Ossenkopf, 1993), a model of a heterogeneous mixture in volume or aggregates would be more accurate for larger particles. A number of authors who used mainly the core-mantle models reported some possible clues to solving this problem (Tielens *et al.*, 1991; Dartois, 2006). Nevertheless, in view of the fact that the laboratory measurements are generally carried out for CO ice deposited on flat substrate (ice films) and given that spectral measurements of ice particles are very scarce and generally applied only to aerosols (Dartois and Bauerecker, 2008; Bauerecker and Dartois, 2009), our comparison of observations and laboratory measurements does not include the effects of the external shape, the size, the internal structure (different components), and the size and shape distributions. These parameters, altogether, are included in the ice spectral observations of dust grains.

We proceeded by separating the influence of each mentioned parameter. In this paper, as starting point, we have mainly considered the influence of the external shape of the dust grains on the CO ice stretching mode. To do this, our calculations only consider ices as the constituent (mainly CO); in the last section, we have included silicate in some aggregates in an attempt to study the influence of the internal structure of the dust grains. In Section 2, we consider ice spheres that range in size from the Rayleigh regime to larger sizes and calculate the extinction factors at low temperature not only for the CO ice stretching mode but also for two bands of the CO_2 ice at 2345 and 657.8 cm^{-1}. In Section 3, we calculate the extinction factors of the CO ice stretching mode for CO ice particles with different shapes: (1) sphere; (2) ellipsoid with axis ratio of 5; (3) the so-called irregular shape DW1996; (4) five aggregates randomly generated with a radius monomer of 0.17 μm for different X up to 3. Additionally, we consider other aggregates with X and monomer radius of 1 and 0.1 μm, respectively. In Section 4, we include silicate as a constituent, randomly changing the refractive index of the 25% of the dipoles of some of the aggregates. Finally, in Section 5, we discuss the results and indicate future calculations.

2. Calculations with Spheres

We have calculated the extinction factors by using Mie code (Mätzler, 2002) for ice spheres considering several bands (the stretching mode of CO ice at 2140 cm^{-1}, the ν_3 stretching mode of CO_2 ice at 2345 cm^{-1}, and the bending mode of CO_2 ice at 657.8 cm^{-1}) from the Rayleigh regime ($X < 1$) to the scattering regime ($X > 1$). The optical con-

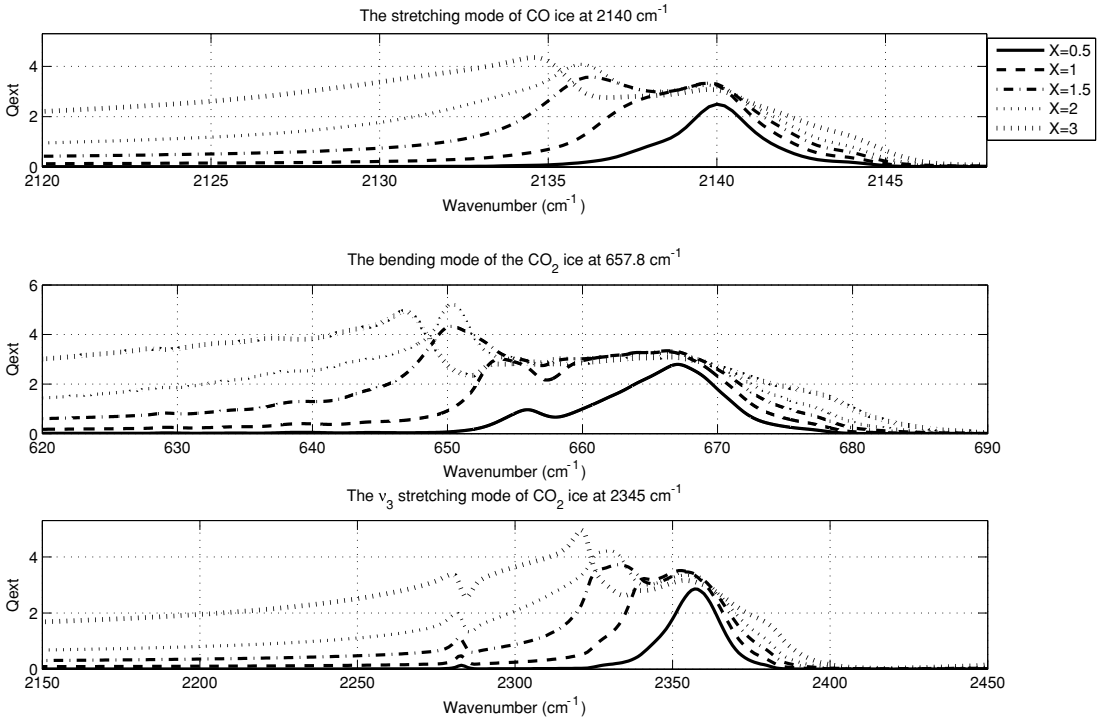

Fig. 1. The extinction factors of the 2140 cm^{-1} band of the CO ice sphere (upper) and 657.8 and 2345 cm^{-1} bands of CO_2 ice sphere (middle and lower) versus the wavenumber for values of X of 0.5, 1, 2, and 3.

stants used for the calculations with CO ice were those obtained by Palumbo *et al*. (2006) with a resolution of 1 cm^{-1} at a temperature of 15 K; the two bands of CO_2 ice were those obtained by Baratta and Palumbo (1998) with a resolution of 2 cm^{-1} at temperature of 12.5 K. Figure 1 shows the results of these three mentioned bands for X values of 0.5, 1, 1.5, 2, and 3, respectively. A typical profile of these bands is observed for $X < 1$; however, when the values of X increase, a broader scattering peak starts to be observed towards the higher wavelengths for the three bands considered. We have compared the absorption factors of the stretching mode of CO ice in the Rayleigh regime with the absorption spectra of pure CO ice deposited on a flat substrate and observed a similar profile. However, in the case of spheres, the band is slightly displaced to higher wavelengths. In other words, our calculations with spheres of CO and CO_2 ice show that grain growth leads to the appearance of a large component displaced to larger wavelengths.

3. Calculations with Other Shapes

Using DDA code (Draine *et al*., 2008) we have calculated the extinction factors of the CO ice stretching mode considering other shapes: (1) ellipsoids with an axis ratio of 5; (2) the so-called irregular shape DW1996; (3) some aggregates randomly generated with spheres of a radius monomer of 0.17 μm. The particle labeled DW1996 consists of an assemblage of 13 cubic units (Draine and Weigartner, 1996), and we have selected this non-realistic shape only for testing the results with different irregular shapes.

For the generation of the aggregates, we performed a Fortran implementation of both a particle-cluster aggregation (PCA) and a cluster-cluster aggregation (CCA) method. The PCA process starts with a single sphere in a fixed position. A new sphere is then attached to it in a random direction. From there on, the new monomers are added to any of the existing ones. A new sphere is then added to it in a random direction, and we checked that the new monomer does not overlap any of the previously added monomers. If it does, the last aggregated sphere is removed, and a new attempt to aggregate a non-overlapping monomer is performed. In the case of the CCA method, we build several PCA clusters and then join them in the following way: we set one of the clusters in the origin, and we put another one far away from the first (in such a way that they do not overlap), in a random direction. We then have the second cluster approach the part of the aggregate that is already formed, until the two touch. For both PCA and CCA, the coagulation process is completed when the maximum distance between any pair of monomers of the aggregate exceeds a certain upper limit. This criterion is realistic because a limitation in the size of an aggregate is given by the maximum length of the particle in a direction perpendicular to the rotation axis: the larger this length is, the larger the centrifugal force becomes for the monomers at the edge. As the force holding the monomers together is constant, aggregates break as a consequence of rotation when they exceed a certain size.

For the DDA calculations, we have used 500 orientations and the principal axis of the moment of the inertia tensor to carry out the calculations in the case of more elongated particles. Figure 2 shows a comparison between the extinction factors calculated for spheres, spheroids of axis ratio 5, the DW1996 particle, and five aggregates of spheres for specific values of X ranging from 0.2 to 3. Figure 3 shows an image of the five aggregates considered with $X = 0.5$, 1, 1.5, 2, and 2.5, respectively, from left to right.

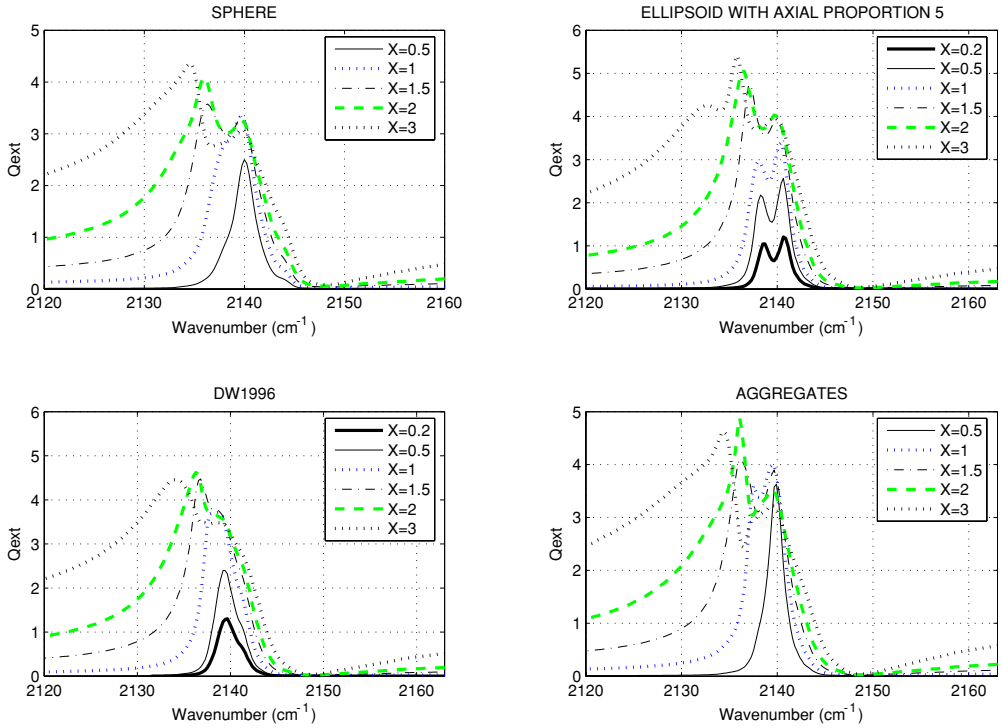

Fig. 2. Comparison of the extinction factors of the 2140 cm^{-1} CO ice band for four shapes: sphere (top left), ellipsoid with axis ratio of 5 (top right), DW1996 (bottom left), and aggregates randomly generated with radius monomer of 0.17 μm (bottom right) from X ranging from 0.5 to 4.

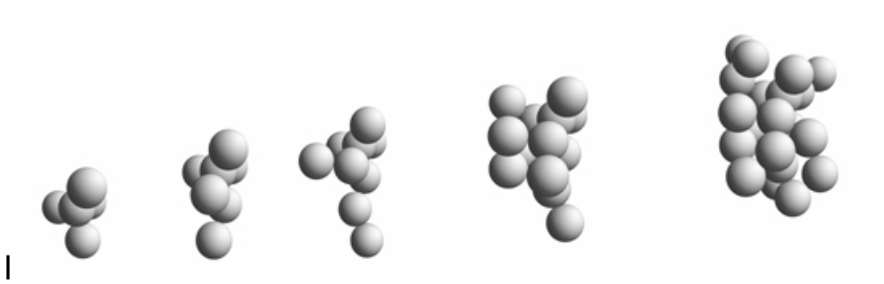

Fig. 3. An image of five aggregates randomly generated with a radius monomer of 0.17 μm. The size parameters of each aggregate are 0.5, 1, 1.5, 2, and 2.5, respectively (from left to right).

These were randomly generated with the PCA method with a size monomer of 0.17 μm. Our results with spheroids of axis ratio 5 clearly show that the double-peaked profile is in accordance with those obtained in the Rayleigh regime by Tielens and co-workers (1991). These subpeaked profiles have been attributed to the surface modes (Boren and Huffman, 1983; Tielens *et al.*, 1991). In our calculations, this substructure remains until $X = 1$, and for this reason, in Fig. 4, we show a comparison of the extinction factors of four different shapes with $X = 1$: (1) the sphere, (2) the spheroid of axis ratio 5, (3) the so-called DW1996 shape, and (4) the second aggregate in Fig. 3 from left to right. From this comparison, it can be easily seen that the double-peaked profile also appears for the aggregate. In an attempt to consider a more realistic monomer size and focusing our attention on aggregates of $X = 1$, we have set the monomer size to 0.10 μm in accordance with the values indicated by a number of authors in their cometary dust models (Brownlee *et al.*, 1980; Greenberg and Hage, 1989; Kimura *et al.*, 2003) and with the results of the Stardust mission (Hörz *et al.*, 2006) and generated two new aggregates using the CCA method. These new aggregates are fluffier than those obtained with the PCA technique. Figure 5 shows an image of these two aggregates, and Fig. 6 shows the extinction factors of these aggregates compared with that obtained for a sphere of $X = 1$; both profiles are almost equal and quite close to that obtained for a sphere.

4. Calculations Including Silicate

In order to include silicate as constituent, we have randomly changed the refractive index of 25% of the dipoles. According to Dorschner *et al.* (1995), the refractive indices of the silicate can be considered equal to $1.81+0.02i$ at each wavelength of CO ice stretching mode. Figure 7 shows four plots, with each one representing a comparison of the extinction factors obtained in two cases: (1) a mixture of the 75% of CO ice and the 25% of silicate; (2) pure CO ice. Each plot represents the results with the aggregates shown in Fig. 3 (excluding the biggest one) with X values of 0.5, 1, 1.5, and 2. As can be seen, the band strengths of the aggre-

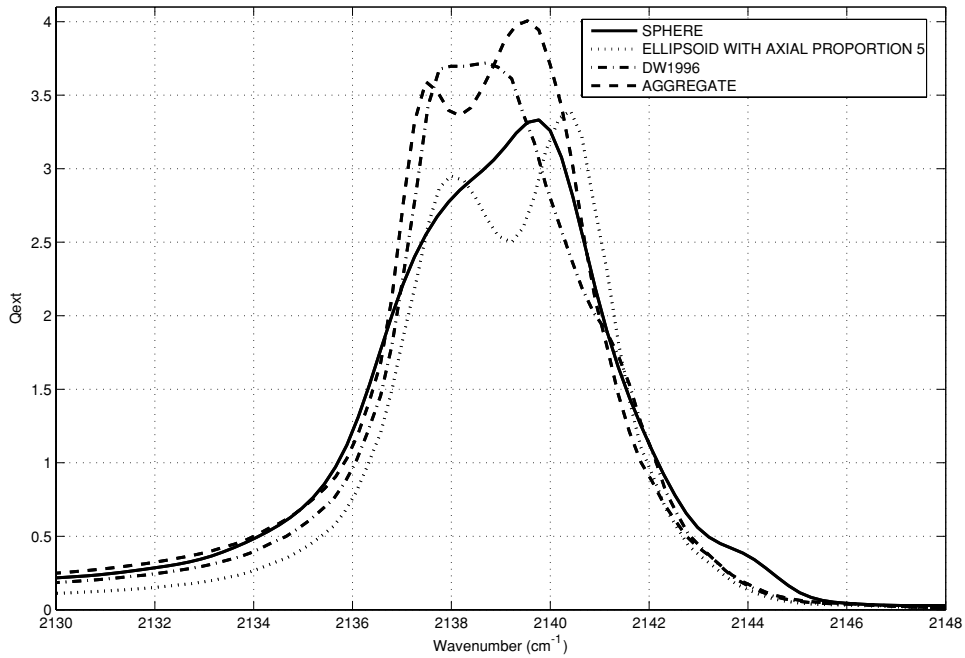

Fig. 4. A comparison of the extinction factors for the four shapes with $X = 1$: a sphere (solid line), an ellipsoid with axis ratio 5 (dotted line), the so-called irregular particle DW1995 (dotted-dashed line), and an aggregate (dashed line).

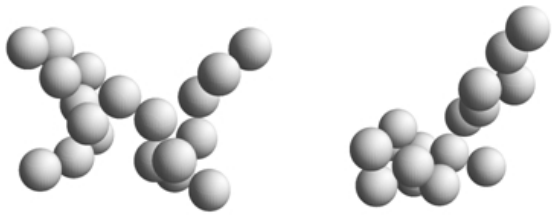

Fig. 5. An image of two randomly generated aggregates. The radius of the monomer was set to 0.1 μm and the X of the particles equal to 1.

gates, including silicate, are lower than those of the pure CO ice in all plots. The plots obtained for X values of 1.5 and 2 also show the rising scattering peak whose strength does not seem to be affected by the inclusion. Finally, in the case of the aggregate with $X = 1$ the double-peaked profile remains, although the subpeaked strength is less pronounced.

5. Discussion and Future Work

Here, we summarize and discuss our results taking into account the fact that the main objective of this study was to shed some light on how the profile of the stretching mode of CO ice is affected by the external shape of the dust grain its size. We have also considered the problem of how this profile can be affected by the internal structure of the particles, including silicate in several of the aggregates we have considered.

In terms of the size effect, we want to highlight the fact that a scattering peak displaced towards the reddish wavelength for X values larger than 1 has been observed in all cases, independently of the ice (CO and CO_2), the shape (sphere, spheroid with axial proportion 5, DW1999, and aggregates), or the inclusion of other constituents, such as silicate. In three of the papers previously mentioned (Tielens *et al.*, 1991; Dartois, 2006; Dartois and Bauerecker, 2008), the authors also reported this observation. These results imply that the grain growth could be the origin of the reddish CO ice stretching mode component observed from many lines of sight provided it is observed somewhere in the range of 2130–2138 cm^{-1}. However, if a double-peaked profile is observed between 2138 and 2145 cm^{-1}, its origin could lie elsewhere (see the explanation below).

With respect to the effect of the external shape of the particle, our results with CO ice ellipsoids with an axis ratio of 5 and with CO ice aggregates (with or without silicate) up to X values of 1 have shown a double-peaked profile between approximately 2138 and 2145 cm^{-1}. This substructure was also observed by Tielens *et al.* (1991) and Dartois and Bauerecker (2008) when they considered different shapes in their calculations with only CO ice. These authors attributed this substructure to the surface modes. The surface modes are easily observed in the Rayleigh regime where the applied fields polarize the particle and where, despite the neutrality of the particle, a charge distribution that depends on the shape is established on the surface. Moreover, the CO ice stretching mode is a strong absorption, and the real part of its dielectric constant varies considerably

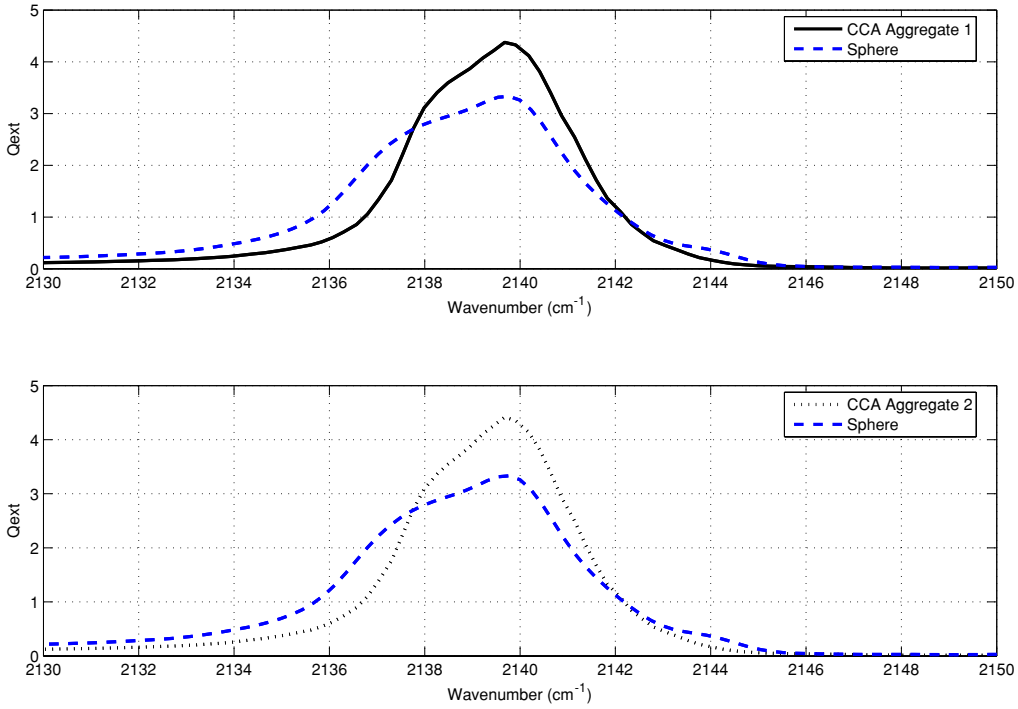

Fig. 6. Comparison of the calculated extinction factors of the aggregate 1 (solid line) and aggregate 2 (dotted line) in Fig. 5 and the extinction factors obtained with a sphere (dashed line) of about $X = 1$.

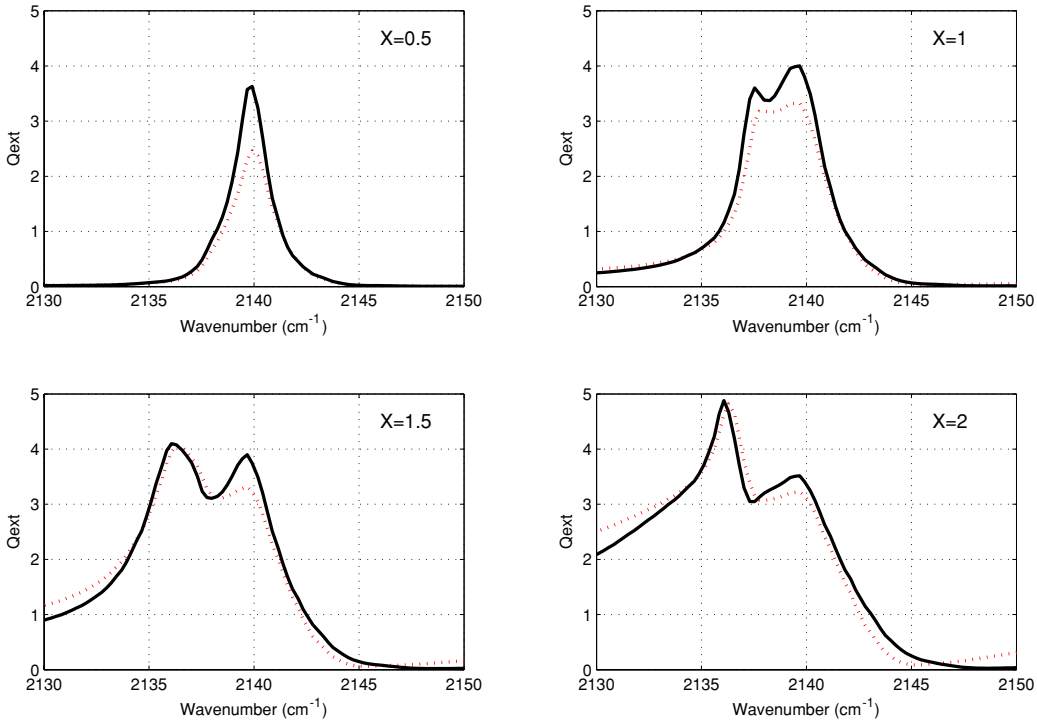

Fig. 7. The extinction factors of CO ice stretching mode for four of the aggregates shown in Fig. 3 with X values of 0.5 (upper left), 1 (upper right), 1.5 (bottom left) and 2 (bottom right) and monomer radius of 0.1 μm, including a 25% of the silicate (dotted line) compared with the results previously obtained for these aggregates without silicate (solid line).

in the neighborhood of this absorption, becoming negative. The surface modes are only important when the real part of the dielectric constant becomes negative (Tielens *et al.*, 1991). The real part of the dielectric constant of the CO ice according to values used in this paper is negative between 2138 and 2145 cm^{-1}. On the other hand, Dartois and Bauerecker (2008), in their experimental and computational studies of the IR spectra of crystalline CO ice clusters in aerosol phase, observed numerous substructures in the profiles of CO ice stretching mode, but these were always between the LO and TO modes. Pontoppidan *et al.* (2003) suggested that the blue component can possibly be

explained by the LO component of the vibrational transition in pure crystalline CO ice, which appears when the background source is linearly polarized. In other words, the external shape effect is a consequence of the surface modes, and the substructure and the relative subpeak strength depend on the shape (prolate versus oblate) but also on the crystalline-amorphous phase.

The problem of the effect of the internal structure of the dust grains is more complicated. A number of authors (Tielens *et al*., 1991; Dartois, 2006) using the core-mantle model observed a double-peaked profile for a relative core-mantle volume fraction of less or equal than 1 (approximately 25% ice) as a consequence of the interface. Dartois (2006) also carried out calculations that included silicate in a volume (ellipsoid) and a relative volume fraction of 1, using the Bruggeman or Looyenga EMT. However, in this case, he only observed one peak. In this paper, we have paid special attention to the aggregates in which we have included silicate, changing randomly the refractive index of the 25% of the dipoles. Our calculations have shown variations in the band strength, but there were no significant changes in the profile. In this case, we are speaking about dipoles in terms of DDA. The calculations with the EMT have the restriction that the inclusions must be Rayleigh; if the inclusions are not dipoles in DDA terms, the scattering characteristics are not well reproduced by the EMT calculations. Therefore, in order to consider non-Rayleigh inclusions, it would be interesting to change the refractive index dipoles surrounding each one.

In terms of our calculations with aggregates, we have considered radius monomers of 0.1 and 0.17 μm and described the PCA and DDA techniques. Our results with aggregates are not sufficient to enable definitive conclusions; however, they do provide clues on the directions of future studies. For example, the fact that an aggregate with $X = 1$ and radius monomer of 0.17 μm gives a double-peaked profile that does not appear with aggregates of the same size parameter but with a radius monomer of 0.1 μm indicates that the radius monomer could be a parameter influencing the appearance of the features on the CO ice stretching mode profile. We are planning to carry out calculations from the Rayleigh to scattering regime with different aggregates (compact, fluffier), including silicate or carbonaceous material.

With respect to mixtures of CO ices, Tielens *et al*. (1991) stated from their experimental measurements with CO ice mixtures on a flat substrate that a mixture dominated by CO (CO concentration $>$ 30%), compared to calculations with spheres of the same ice mixtures, shows shifts in the peak position and variations of the band wideness of a few wavenumbers. At lower concentrations, laboratory spectra represent the calculated ones very well. Therefore, it would be interesting to perform computational calculations for mixtures in which the percentages of the CO ice was less or greater than 30%. The wideness and position of the middle or dominant component of the CO ice stretching mode is observed to vary from object to object.

To sum up, given that the so-called red component is broader, red-shifted, and situated somewhere in the region of 2130–2138 cm^{-1}, the red component observed from many lines of sight seems to be related to the grain growth. However, despite the average in shapes and sizes tending to smooth the spectral substructure, if a doubled-peaked profile is observed in the range of 2138–2145 cm^{-1}, it could be the consequence of the shape or internal structure of the dust grain (i.e., core-mantle particles or preponderance of certain shape), given the knowledge that core/mantles volume ratios also smooth out the multiple peaks.

Acknowledgments. This work was supported by contract AYA2007-63670, AYA2007-65899, and FEDER funds.

References

Baratta, G. A. and M. E. Palumbo, Infrared optical constants of CO and CO_2 thin icy films, *J. Opt. Soc. Am.*, **15**, 3076–3085, 1998.

Bauerecker, S. and E. Dartois, Ethane aerosol phase evolution in Titan's atmosphere, *Icarus*, **199**, 564–567, 2009.

Boren, C. F. and D. R. Huffman, *Absorption and Scattering of Light by Small Particles*, pp. 325–380, Wiley Science Paperback Series, 1983.

Brownlee, D. E., L. Pilachowski, E. Olszewski, and P. W. Hodge, Analysis of interstellar dust collections, in *Solid particles in the solar system*, *Proceedings of the Symposium, Ottawa, Canada*, pp. 333–342, 1980.

Dartois, E., Spectroscopic evidence of grain ice mantle growth in YSOs I. CO ice modeling and limiting cases, *Astron. Astrophys.*, **445**, 959–970, 2006.

Dartois, E. and S. Bauerecker, Infrared analysis of CO ice particles in the aerosol phase, *J. Chem. Phys.*, **128**, 154715, 2008.

Dartois, E., L. D'Hendecourt, W. F. Thi, K. Pontopiddan, W. A. Schutte, and E. F. van Dishoeck, Ices and gas in star forming regions as seen with VLT-ISAAC spectroscopy, in *galactic star formation across the stellar mass spectrum*, *Conference Series*, pp.187–192, 2003.

Dorschner, H., B. Begemann, T. Henning, C. Jaeger, and H. Mutschke, Steps toward interstellar silicate mineralogy. II. Study of Mg-Fe-silicate glasses of variable composition, *Astron. Astrophys.*, **300**, 503–520, 1995.

Draine, B. T. and J. C. Weigartner, Radiative torques on interstellar grains. I. Superthermal spin-up, *Astrophys. J.*, **470**, 551–565, 1996.

Draine, B. T. and P. J. Flatau, User guide for the Discrete Dipole Approximation code DDSCAT.7.0, 2008.

Ehrenfreund, P., A. C. A. Boogert, P. A. Gerakines, D. J. Jansen, W. A. Schutte, A. G. G. M. Tielens, and E. F. van Dishoeck, Laboratory database of solid CO and CO_2 for ISO, *Astron. Astrophys.*, **315**, 341–344, 1996.

Ehrenfreund, P., A. C. A. Boogert, P. A. Gerakines, A. G. G. M. Tielens, and E. F. van Dishoeck, Infrared spectroscopy of interstellar apolar ice analogs, *Astron. Astrophys.*, **328**, 649–669, 1997.

Fama, M. A., M. J. Loeffler, U. Raut, and R. A. Baragiola, Radiation-induced amorphization of crystalline ice, *American Astronomical Society, DPS meeting*, 2008.

Geballe, T. R., Absorption by solid and gaseous CO towards obscured infrared objects, *Astron. Astrophys.*, **162**, 248–252, 1986.

Greenberg, J. M. and J. I. Hage, From interstellar dust to comets: A unification of observational constraints, *Astrophys. J.*, **361**, 260–264, 1989.

Hörz, F. and coauthors, Impact features on Stardust: Implications for comet 81P/Wild 2 Dust, *Science*, **314**, 1716–1719, 2006.

Hudgins, D. M., S. A. Sandford, L. J. Allamandola, and A. G. G. M. Tielens, Mid- and Far-infrared spectroscopy of ices: optical constants and integrated absorbencies, *Astrophys. J. Suppl. Ser.*, **86**, 713–870, 1993.

Kimura, H., L. Kolokolova, and I. Mann, Optical properties of cometary dust. Constraints from numerical studies on light scattering by aggregate particles, *Astron. Astrophys.*, **407**, L5–L8, 2003.

Lacy, J. H., F. Baas, L. J. Allamandola, C. E. P. van de Bult, S. E. Persson, P. J. McGregor, C. J. Lonsdale, and T. R. Geballe, 4.6 micron absorption features due to solid phase CO and cyano group molecules toward compact infrared sources, *Astrophys. J.*, **276**, 533–543, 1984.

Mätzler, C., MATLAB functions for Mie scattering and absorption, *Institut für Angewandte Physik, Research Report No. 2002-08, Bern, Switzerland*, 2002.

Ossenkopf, V., Dust coagulation in dense molecular clouds: The formation of fluffy aggregates, *Astron. Astrophys.*, **280**, 617–646, 1993.

Palumbo, M. E., Formation of compact solid water after ion irradiation at 15 K, *Astron. Astrophys*, **453**, 903–909, 2006.

Palumbo, M. E., A. G. G. M. Tielens, and A. T. Tokunaga, Solid Carbonyl Sulphide (OCS) in W33A, *Astrophys. J.*, **449**, 674–680, 1995.

Palumbo, M. E., G. A. Baratta, M. P. Collings, and M. R. S. McCoustra, The profile of the 2140 cm^{-1} solid CO band on different substrates, *Phys. Chem. Chem. Phys.*, **8**, 279–284, 2006.

Pontoppidan, K. M., H. J. Fraser, E. Dartois, W. F. Thi, E. F. van Dishoeck, L. d'Hendrcourt, A. G. G. M. Tielens, and S. E. Bisschop, A 3-5 μm VLT spectroscopic survey of embedded young low mass stars I. Structure of the CO ice, *Astron. Astrophys.*, **408**, 981–1007, 2003.

Raut, U., M. J. Loeffler, R. A. Vidal, and R. A. Baragiola, The OH stretch infrared band of water ice and its temperature and radiation dependence, *Lunar Planet. Sci. Conf.*, 2004.

Schmitt, B., J. M. Greenberg, and R. J. A. Grim, The temperature dependence of the CO infrared band strength in CO: H_2O ices, *Astrophys. J.*, **340**, 33–36, 1989.

Smith, R. G., G. Robinson, A. R. Hyland, and G. L. Carpenter, Molecular ices as temperature indicators for interstellar dust: the 44 and 62 μm lattice features of H_2O ice, *Mon. Not. Roy. Astron. Soc.*, **271**, 481–499, 1994.

Tielens, A. G. G. M., A. T. Tokunaga, T. R. Geballe, and F. Baas, Interstellar solid CO: polar and nonpolar interstellar ices, *Astrophys. J.*, **381**, 181–199, 1991.

Whittet, D. C. B., A. D. McFadzean, and A. J. Longmore, Solid CO in the Taurus dark clouds, *Mon. Not. Roy. Astron. Soc.*, **216**, 45P–50P, 1985.

R. Vilaplana (e-mail: rovilap@fis.upv.es), J. Canto, F. Moreno-Danvila, and D. Guirado